Solid State Phenomena Vols. 85-86 (2002) pp 317-336
© (2002) Trans Tech Publications, Switzerland
doi:10.4028/www.scientific.net/SSP.85-86.317

Ultrasound Stimulated Defect Reactions in Semiconductors

Sergei Ostapenko[1], Nadejda E. Korsunskaya[2] and Moissei K. Sheinkman[2]

[1] Center for Microelectronics Research, University of South Florida,
4202 E Fowler Avenue, Tampa FL 33620, USA

[2] Institute of Semiconductor Physics, National Academy of Sciences,
45 Prospect Nauki, Kiev 252028, Ukraine

Keywords: Dislocations, Gettering, Hydrogen, Photoluminescence, Ultrasound

Abstract. Ultrasonic vibrations introduced into semiconductors can trigger defect reactions, which are beneficial for electronic materials and devices. This type of semiconductor processing is referred to *ultrasound treatment (UST).* UST technology was initially developed in compound semiconductors and recently successfully applied to Si based materials. The analysis of UST effects is performed within a general scenario of the three-step point defect gettering comprised of (a) the release, (b) diffusion, and (c) capture of defects. As a demonstrating vehicle of UST mechanisms, the experimental data on ultrasonically enhanced diffusion of the atomic hydrogen in thin polycrystalline Si films and dislocation gettering in II-VI semiconductors are discussed. In the first case, the mechanism of trap-limited hydrogen diffusion facilitated by the ultrasound was proposed. Illustrative examples of the UST application for electronic devices are presented.

Introduction

Discovered in the late 60's and extensively explored since 80's [1], the ultrasound stimulated processes in Ge, Si, and compound semiconductors attracted the attention of various research groups. It has been demonstrated that ultrasonic vibrations generated into crystal can stimulate numerous defect reactions and, as a consequence, benefit a design of electronic materials with improved and even superior characteristics. This new technological approach has become a powerful tool of the defect engineering to improve performance and reliability of microelectronics devices.

Ultrasonic processing of semiconductors and relevant mechanisms are referred to Ultrasound Treatment (hereafter the UST). UST effect can be defined as a stable improvement of material properties and device parameters after they have been affected by the ultrasound. The UST method utilizes a fundamental concept in solids. It is based on a coupling of the ultrasonic vibrations with a system of point defects, both of impurity and native origin, interacting with the extended defects such as dislocations, grain boundaries, and precipitates to control their physical properties, and to improve defect related material parameters. Therefore, UST realizes a method of defect engineering in semiconductors to benefit material quality. UST method is based on a solid and well-understood physical concept. Crystal defects and their complexes can exist in a stable, unstable or metastable configuration. A bottom line of UST technology is that mechanical vibrations can assist a system of crystal defects in reaching a favorable position, which has the lowest total energy; therefore, this is the preferable, stable state. As a consequence, material properties and device parameters become more stable preventing or diminishing the aging or degradation. Important that a positive UST effect

can be achieved by a careful optimization of an ultrasonic regime (temperature, amplitude, frequency and duration) specific for individual material or device. On the other hand, UST is a simple and intuitive approach. Many people may be experienced with a simple "ultrasound treatment" in their daily routine without noticing it. The following illustrative "case" reveals the utility of mechanical vibrations to solve a simple problem.

Gas bubbles in a liquid. Imagine if you decided to have a drink of soda and are trying to get rid of the gas-bubbles, which are strongly attached to the glass walls, before you drink it. Knock with your finger on the glass and immediately some of these "tough" bubbles will be released and run to the surface. What happened? The acoustic vibrations were generated in the glass and transferred their energy to bubbles. This extra energy was enough to release trapped bubbles by breaking their molecular bonds of surface tension with the glass. This simple example is surprisingly similar to what the ultrasound is doing to enhance defect passivation with hydrogenation in poly-Si films, a material for a new generation of active-matrix-liquid-crystal-displays. It will be shown in section 2A, that trapped atomic hydrogen can be released by UST and moved to "proper" positions at dangling bonds, which benefit transport properties of electrons and holes. This process can eventually improve thin-film transistor's leakage current and threshold voltage: critical parameters of transistor's application.

This article describes the UST method and apparatus, and also summarizes UST controlled defect reactions, relevant mechanisms, and application issues. Particular examples: dislocation gettering in II-VI semiconductors and enhanced hydrogenation in poly-Si thin films provide a deeper insight into specific UST mechanisms.

1. UST method and apparatus

Ultrasonic vibrations have to be delivered to a semiconductor materials or electronic device to perform UST processing. Three different techniques to generate ultrasonic vibrations are applicable.

(1) The most general method utilizes an external source of ultrasound, such as a resonance piezoelectric transducer. This UST technique has advantages of a non-contact processing in an active device region at the front surface of wafer and applicable for large-scale materials and devices, such as 8" Si-wafers and more than 12" flat-panel-displays. This UST approach is also compatible with conventional device processing steps: deposition, annealing, doping, and passivation. A schematic of the UST unit - key element of a large-scale UST station - is shown in Figure 1. Low-amplitude ultrasonic vibrations are generated into the UST object: a semiconductor wafer, thin film on a substrate, or a microelectronics device using a piezoelectric transducer operating in a resonance vibration mode and coupled with the UST object. Typically, a circular transducer is driven by a generator and power amplifier adjusted to the first resonance of its radial or thickness vibrations. The resonance frequency varies from 20KHz to 100KHz for radial vibration mode and can be extended in MHz-range using thickness vibrations. This frequency depends on transducer geometry, vibration mode, material of a piezoelectric transducer, and varies with UST temperature and amplitude. Adjusted to a resonance frequency, the UST transducer generates a maximum ultrasonic amplitude, which is quantified by the value of acoustic strain. The amplitude of acoustic strain is the ratio of vibrating amplitude to the characteristic size of the transducer (e.g. diameter). In UST technique, the acoustic strain does not typically exceed 10^{-4} corresponding to the acoustic power of a few W/cm^2. To provide an effective UST processing, the acoustic strain is controlled with a calibrated sensor of acoustic vibrations (non-contact UST probe). The UST temperature can be stabilized from room temperature up to the Curie point of the transducer (350^0C for commercial PZT-5A piezoceramics). A sample has to be placed on a UST chuck composed of one or more UST

transducers and tightly pressed against a chemically polished transducer surface using a vacuum contact. A computer system controls "in-situ" and adjusts UST parameters: amplitude, frequency, and temperature operating in a feedback loop with the non-contact UST probe and non-contact infrared temperature sensor. This approach has been realized in a multi-transducer UST station, which is capable of processing large-scale wafers by delivery of a quasi-homogeneous distribution of UST amplitudes and temperature from a set of UST transducers to the 12" diagonal samples [2]. The station can be scaled up simply by adding ultrasound transducers to a custom designed configuration of the UST chuck.

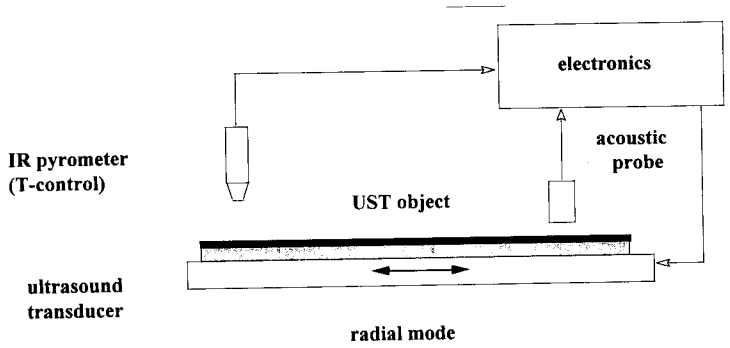

Figure 1. Schematic of ultrasound treatment unit for UST processing of semiconductor materials and devices.

(2) UST vibrations can alternatively be generated into a material using the internal piezoelectric effect of a semiconductor. In this case, the ac voltage is applied via electrodes oriented along specific crystallographic directions (e.g. along the C axis in a hexagonal-type crystal). The ac electric field generates intensive ultrasonic vibrations when its frequency (between 100KHz and 20MHz) is adjusted to the acoustic resonance of a sample. This method is limited to semiconductors with a high resistance possessing a noticeable piezoelectric constant (CdS, CdSe, $CdZnP_2$, and others). It also requires a special sample shaping in the form of an acoustic resonator [3].

(3) Another UST approach is based on pulse light absorption. The absorption in a metal foil attached to crystal surface of a nano-second laser pulse (e.g. a ruby laser with a power density of the order 10^9 W/cm^2) generates a set of ultrasonic pulses [4]. These ultrasonic vibrations can be coupled with crystal defects and perform an effective UST processing. In this technique, laser density of power has to be carefully controlled to prevent the degradation of a material due to creation of new crystal defects.

2. Fundamental: UST phenomena and mechanisms

Although UST effects in semiconductors are well documented, there are a limited number of conclusive results where a clear understanding of relevant physical mechanisms was achieved. In Table 1, we classified UST mechanisms proposed in various semiconductor materials. The key UST experiments, illustrating specific topics, will be discussed in detail.

Table 1. Ultrasound stimulated processes in semiconductors

Physical mechanism	Material	Reference
A. Dissolving of defect clusters and pairs	Poly-Si	[5,6]
	Cz-Si	[7]
	CdHgTe	[8]
	CdS	[9]
	GaAs	[10]
B. Enhanced diffusion	Ge	[11]
	Si	[12,13]
	CdS	[4]
C. Capture of point defects	CdS	[14]
	CdTe	[15,16]
	ZnCdTe	[17]
	CdSSe	[18]

UST mechanisms are tightly related to processes of point defect gettering and passivation. Defect gettering was introduced into semiconductors using a terminology of the cathode-ray-tubes (TV screens) where the gettering technique is successfully applied to improve long-term vacuum characteristics of a tube with gas-absorbers. In silicon microelectronics, a similar but essentially more sophisticated approach provided a development and progress of Si-wafers with contamination level below than 10^{11} cm^{-3}. There are two general ways to achieve a high device yield and reliable device performance in microelectronics technology. The first one requires a top-quality starting material, which has to be processed further under an extremely clean fab environment. This is potentially a superior approach but at present is not a realistic one. The second approach suggests the use of various defect-engineering tools, particularly gettering and passivation to grow starting wafers with a moderate contamination level and to achieve a high-quality final product - the IC chip.

According to a general gettering strategy, the gettering process is comprised of three consecutive steps, illustrated in Fig.2. First, a contamination impurity (Fe, Cu, Cr) introduced during wafer/device processing in a device region near the front surface of a wafer has to be released from the bound state. Secondly, a released impurity is diffusing due to the concentration gradient toward the gettering sites (sinks) which are typically placed far away from the device region (e.g. at the

backside wafer surface). At the last step, contamination atoms have to be captured at crystallographic defects or bound with other chemical elements at the gettering sites.

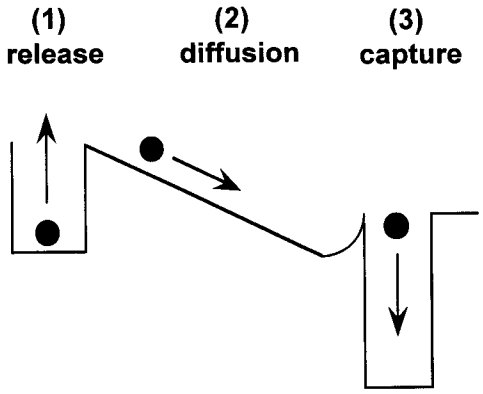

Figure 2. Concept of three-step gettering developed in semiconductor silicon.

A very similar scenario has to be realized for effective passivation of defects using atomic hydrogen. It was found that UST processing can positively affect each of three gettering/passivation steps: release, diffusion and capture as will be illustrated hereafter.

2A. Dissolving of defect clusters: hydrogenation enhancement in poly-Si.

Polycrystalline silicon (poly-Si) thin films on glass or fused silica substrates are promising for thin film transistor (TFT) technology in active matrix liquid crystal displays. Compared with transistors using amorphous silicon films, poly-Si TFTs have improved operational parameters due to a substantially higher electron mobility. However, grain boundary states and interface defects in poly-Si lead to a high off-state current and affect a threshold voltage. A conventional approach to passivate these defect states and to reduce inter-grain barriers for electron transport is to apply plasma hydrogenation. The hydrogen defect passivation occurs in two steps: plasma penetration and subsequent atomic hydrogen diffusion. Unfortunately, the diffusion of hydrogen in poly-Si is slow compared with single crystal silicon due to a trap limiting mechanism at grain boundaries, resulting in a long hydrogenation time (typically an hour at 300^{o}C) and electrical inhomogeneity within passivated regions of poly-Si. This problem motivates a search for non-traditional approaches in order to improve hydrogenation in poly-Si films. It has appeared that the atomic hydrogen in poly-Si thin films is a specifically suitable object for UST process [5]. Based on experiments, the mechanism of UST enhanced liberation of the atomic hydrogen from trapping states was proposed [19]. This UST effect is a "trigger" of fast hydrogen diffusion in poly-Si and ultimately provides an effective passivation of defects at grain boundaries.

For UST experiments, ultrasound vibrations were generated into 0.5μm poly-Si films and thin-film transistors through a glass substrate using a circular 75mm diameter piezoelectric transducer, as shown in Figure 1. The UST transducer operated at about 25kHz resonance of radial vibrations at temperatures ranging from room temperature to 300°C. The UST effect was monitored by measurements of sheet resistance at room temperature using the four-point-probe method. Concurrently, spatially resolved PL and nano-scale contact potential difference mapping were performed.

It was found that conventional plasma hydrogenation applied to poly-Si films reduces sheet resistance up to one order of magnitude due to hydrogenation of grain-boundary dangling bonds. In films where plasma hydrogenation process was not completed, the additional strong reduction of resistance after UST by a factor of ***two orders*** *of* magnitude was observed (Figure 3a). It is important to note that resistance of the non-hydrogenated films was practically unchanged after identical UST.

Another feature of the UST effect is an improvement of resistance homogeneity shown in Fig.3. By monitoring UST changes of resistance in two different regions of the same film with a high starting electrical inhomogeneity, it was found that the initial more than one order of magnitude difference in resistance was reduced to approximately 10% after a few consecutive steps of UST. Based on these findings, it was concluded that ultrasound vibrations applied to hydrogenated films promote a redistribution of the atomic hydrogen. This effect was directly observed by measuring of contact potential difference mapping with spatial resolution of 20nm. The contrast of contact potential mapping originated from the charge states at grain boundaries (non-passivated dangling bonds) was substantially improved after UST [5].

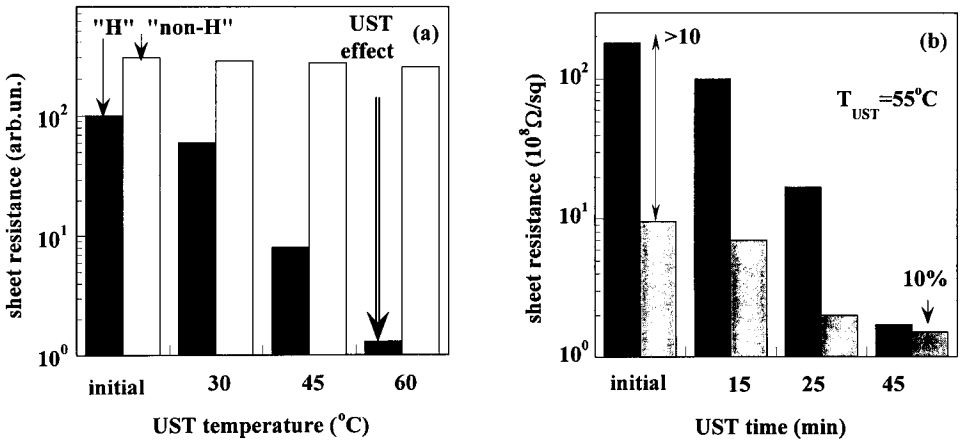

Figure 3. UST reduces resistance (a) and improves homogeneity (b) in hydrogenated undoped poly-Si thin films on glass.

It was reported that photoluminescence (PL) spectroscopy allows defect monitoring in polycrystalline Si films, and is specifically sensitive to the hydrogenation process [20]. At 4.2K the PL band corresponding to band-tail recombination dominates in the luminescence spectrum of films deposited at 625°C (Fig. 4). With increasing temperature, the band-tail emission is strongly quenched and the broad "defect" PL maximum at about 0.65 eV is retained and persists at room

temperature. The "defect" PL intensity can be used to assess the result of hydrogenation and UST processing on the film recombination properties. It was found that "defect" band PL intensity is increased by a factor of 8 after the ECR plasma hydrogenation [20]. This was attributed to the passivation by atomic hydrogen of non-radiative centers: dangling silicon bonds at the grain boundaries, which are competing for the capture of minority carriers injected by an excitation laser beam.

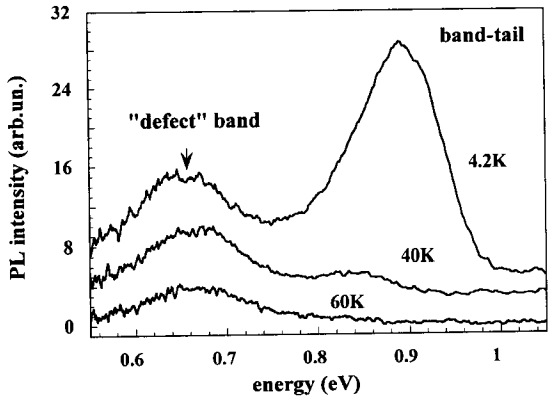

Figure 4. Photoluminescence spectra of poly-Si thin films on glass deposited at 625°C measured at different temperatures. Intensity of the 0.65eV band can be used to monitor quality upgrading of a thin film after hydrogenation and UST.

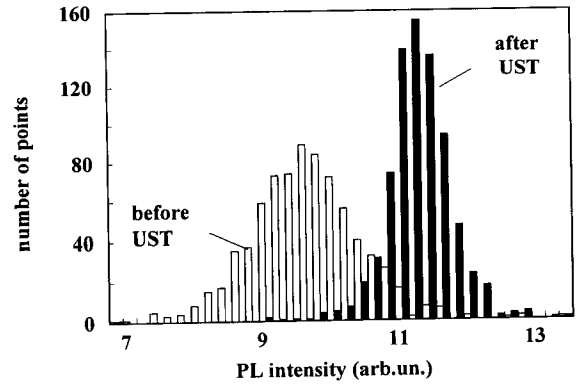

Figure 5. Two histograms of the PL intensity in hydrogenated poly-Si film before and after UST. Compared to hydrogenated sample, UST additionally increases PL intensity due to redistribution of the atomic hydrogen at grain-boundary and passivation of non-radiative defects.

Spatially resolved PL mapping technique with a resolution of 100μm was used to monitor UST changes in distribution of recombination centers. The result is presented in Figure 5 as two

histograms of exactly the same hydrogenated film area prior to and after UST. The average value of PL intensity after UST exhibits an additional 30% increase and a narrowing of the histogram half-width by a factor of two. This result is in excellent agreement with the UST-induced improvement of resistance homogeneity.

It was anticipated that UST is a thermally activated process, which can be facilitated above 100°C. To verify this, poly-Si films thermally recrystallized at 550°C and annealed at the same temperature as long as 75 hours were subjected to UST at temperature up to 280°C [6]. Notice that this material contains a mixture of amorphous (a-Si) and polycrystalline Si phases. A volume ratio of crystalline to amorphous phase was quantitatively measured by Raman spectroscopy. The "defect" band shown in Figure 4 dominates the PL spectrum of poly-Si thin films at 77 K. (Notice a shift of the "defect" band from 0.65 to 0.7eV in some samples). By increasing annealing time of 550°C films up to 75 hours, it was found that the intensity of the defect PL band was monotonously increased by a factor of ten tracking the increase of the polycrystalline fraction. Therefore, the intensity of the 0.65eV band can be used to monitor changes of recombination properties in the poly-Si phase of films.

After UST was applied to 550°C annealed films at T_{UST}=150-280°C, two noticeable changes in PL spectrum were observed (Fig. 6). The first is the increase of the "defect" band intensity by a factor of 2 to 4 (in different samples), which is consistent with the data of low-temperature UST processing of hydrogenated poly-Si films shown in Figure 5. The second and dominant effect is a strong UST activation of a "new" broad PL band with a maximum at 0.98eV and the half-width of 260meV at 77K. This PL band is clearly distinguished from the band-tail luminescence in polycrystalline silicon (see Fig.3), having a different line-shape and temperature quenching. This band is attributed to luminescence defects localized in the amorphous phase of the film. We noticed a dramatic enhancement of 0.98eV band exceeding *two orders* of magnitude, which require only a few minutes of UST processing at 250-280°C. After UST activation of luminescence is completed the PL spectrum is entirely dominated by the 0.98eV band.

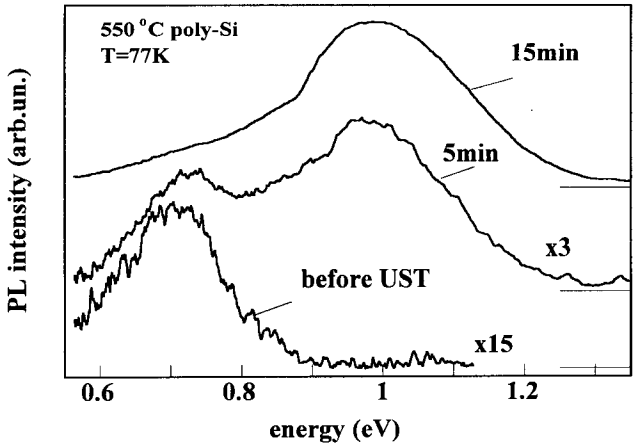

Figure 6. UST applied at temperatures from 150°C to 280°C strongly activates photoluminescence intensity in polycrystalline and amorphous phase of LPCVD thin films deposited at 550°C and annealed at 550°C for 24 hours.

UST processing was performed at different temperatures between 150°C and 280°C. Corresponding points of isothermal kinetics of the 0.98eV band at two temperatures and their single-exponential fits are shown in Figure 7. For a comparison, the picture also comprises PL kinetics of a control sample annealed without UST proving that the effect of the 0.98eV band activation is entirely UST related. From the Arrhenius plot of UST time constant it was found the UST activation energy of E_{UST}=0.33eV. The UST kinetic is characterized by a time constant of 3min at 280°C. Notice, that this rate of UST processing is compatible with the state-of-art plasma hydrogenation of commercial thin film transistors.

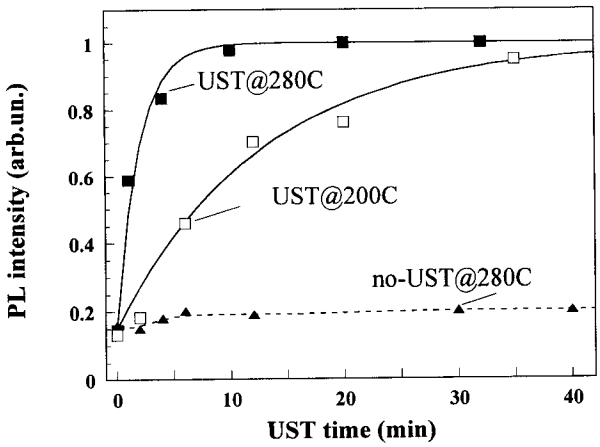

Figure 7. Isothermal kinetics of the 0.98eV PL band activated using UST (points) and exponential fit (curves). Notice that simple annealing at 280°C without UST does not affect PL intensity.

It is known that after plasma hydrogenation the total hydrogen concentration in poly-Si films can exceed the number of non-passivated dangling bonds by as much as two orders of magnitude [21]. Therefore, a significant "reservoir" of electrically non-active hydrogen in trapping states is available after plasma hydrogenation. It is suggested that UST promotes a release of hydrogen from traps (Figure 8). A physical basis of such UST hydrogen detrapping is a selective absorption of the ultrasound by grain boundaries, dislocations, and other extended crystal defects where hydrogen can reside. Being liberated from traps, hydrogen subsequently become a fast diffuser with the diffusion coefficient of crystalline Si: $D_H=9.4\cdot10^{-3}$ x exp (-0.48eV/kT) [cm^2/sec] [22]. In fact, the measured UST activation energy (E_{ust} = 0.33eV) has a value close to the activation of H diffusion in crystalline Si (about 0.48eV). A possible reduction of this energy can be attributed to UST stimulated diffusion of the atomic hydrogen, the UST mechanism discussed in section 2B. The diffusion length of the hydrogen migration under UST (T_{ust}=280°C, Δt=3min) can be estimated as $L=(D_H\ \Delta t)^{1/2}$=76μm. This value substantially exceeds a 100nm grain-size of poly-Si films, which explains why liberated hydrogen atoms can quickly approach the dangling bonds at grain boundaries of poly-Si. The proposed UST model is in remarkable similarity to the case of gas bubbles in a soda trapped on a glass wall and released after shaking off (see the Introduction).

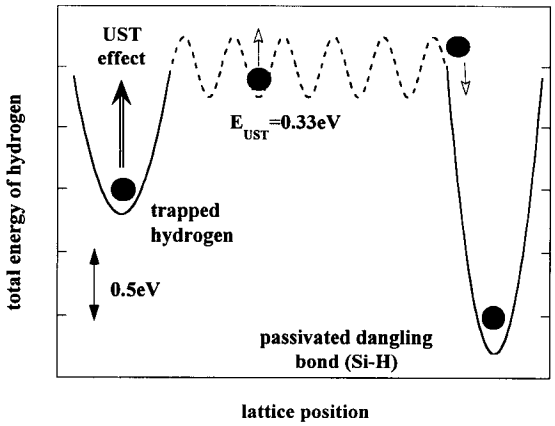

Figure 8. The model of three-step UST enhanced hydrogenation in thin polycrystalline Si films [19]. After UST, the trapped atomic hydrogen is released from electrically non-active state into the bulk (a). The following fast hydrogen diffusion (b) and a capture at grain-boundary defects (c) accomplish UST processing.

The UST processing was applied to hydrogenated poly-Si thin film transistors [23]. The reduction of a leakage current by a factor of 10 and a shift of threshold voltage by as much as 0.5V are consistent with the proposed model of UST enhanced hydrogenation. These experiments demonstrate a utility of UST processing for the improvement of poly-Si active-matrix displays.

2B. Enhanced diffusion: Cr in Cz-Si

Ultrasound accelerated diffusion of point defects was previously observed in metals [24], and later in elemental semiconductors, Ge and Si [11-13]. UST reduces the activation energy of the diffusion process by a few tenths of an electron-volt, and by this means, it facilitates low-temperature defect reactions. This UST effect can positively contribute to a gettering process.

UST enhanced diffusion is related to the multiplication of dislocations described below. In fact, diffusion of substitutional In, Al, and Ga in germanium single crystals was accelerated via a dislocation network [11]. The mechanism is based upon the fact that point defect diffusion is accelerated along the dislocation pipe compared to that in a regular crystal. This can be described by the equation

$$D_{UST} / D_0 = 1 + \pi r^2 N_D D_D / D_v \quad (1)$$

where D_0 and D_{UST} are the diffusion coefficients in the dislocation-free lattice and in UST dislocated crystal; D_D and D_v are the coefficients of diffusion via dislocation and in the volume of a crystal, r is the radius of dislocation pipe ranged from 1nm to 10nm, N_D stands for dislocation density. The ratio D_D / D_v may exceed 10^6 which explains the UST enhancement of point defect diffusion in dislocated materials by a factor of an order of magnitude.

Diffusion of point defects can also be facilitated in a dislocation-free material such as Cz-Si wafers. According to theoretical model [25], the impurity atom absorbs the energy of

nonequilibrium phonons excited by the ultrasound, and this energy increases the rate of impurity migration. Two specific factors contribute to this UST mechanism: (1) the change in population of the impurity quantum oscillator levels due to the interaction of an impurity atom with ultrasonically excited non-equilibrium phonons, and (2) the change of a probability of an impurity migration at a particular quantum level.

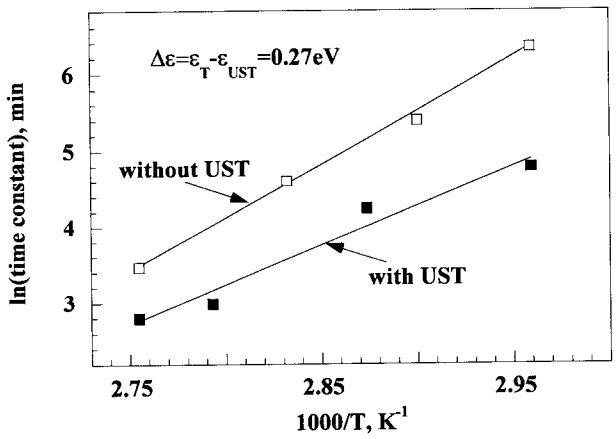

Figure 9 Ultrasound vibrations stimulate low-temperature diffusion of interstitial Cr in Cz-Si. UST reduces the activation energy of Cr diffusion to form Cr-B pairs.

Experiments were performed in p-type boron doped Cz-Si wafers co-doped with chromium (Cr) at the concentrations from 10^{12} to 10^{14} cm^{-3} [13]. In equilibrium, interstitial chromium atoms - Cr_i - form the nearest-neighboring Cr_i-B pairs, which can be dissociated after 200^0C annealing and quenching of Si wafer. The following low-temperature pairing kinetics of Cr_i and B is entirely controlled by the chromium bulk diffusion, which provides a convenient method to measure the low-temperature diffusion constant of the chromium ions. The rate of the Cr_i-B pairing can be measured at different temperatures from room temperature to about 100^0C by monitoring pair concentration via the minority carrier diffusion length as a function of pairing time. The Arrhenius plot shown in Figure 9 represents Cr diffusion data without UST and with UST. Measured in this way the activation energy of Cr_i diffusion without UST of 0.86eV is consistent with published data. It is shown that this activation energy is significantly reduced under UST by 0.27eV. This UST effect can potentially benefit gettering of Cr contamination and improve commercial Si-wafers for IC application.

Another example is revealed by the UST enhanced diffusion of donors in CdS single crystals where the ultrasound was generated with a pulsed laser beam [4]. The effect of shallow donor gettering by dislocations was substantially enhanced and occurred within a microsecond time frame, independent of the UST temperature between 77K and 300K. This was interpreted as extremely low activation energy of point defect diffusion under pulsed UST processing. UST acceleration of point defect diffusion can be applied to different technological problems requiring fast defect reactions.

2C. Capture of point defects by dislocations in II-VI compounds

UST stimulated capture of mobile defects was experimentally observed in different II-VI semiconductors (Table 1). Point defect gettering benefits mechanical, transport, and optical properties of electronic material. The physical origin of UST gettering is a selective absorption of the ultrasound at extended crystal defects such as dislocations, grain boundaries, and precipitates. The energy of absorbed UST vibrations can be coupled with point defects and activate different defect reactions. We consider the vibrating string model of Granato-Lucke to describe a dislocation motion stimulated by the ultrasound [26]. This model is illustrated in Figure 10. Within this model, a dislocation line is considered as an elastic string oscillating between pinning points.

It is assumed that for zero applied stress the dislocations are straight and pinned down by the impurity particles (a). In general, the concentration c of impurity atoms on the dislocation line is larger than the overall concentration c_0 of impurities in the lattice, which is known as a dislocation Cottrell atmosphere. At temperatures T high enough for diffusion to take place, the concentration can attain an equilibrium value according to

$$c = c_0 \exp(Q/kT), \tag{2}$$

where Q is the Cottrell interaction energy between a dislocation and impurity atom. In addition, it is assumed that the interaction of the dislocation with the lattice can be neglected and that interactions between individual dislocations can be neglected.

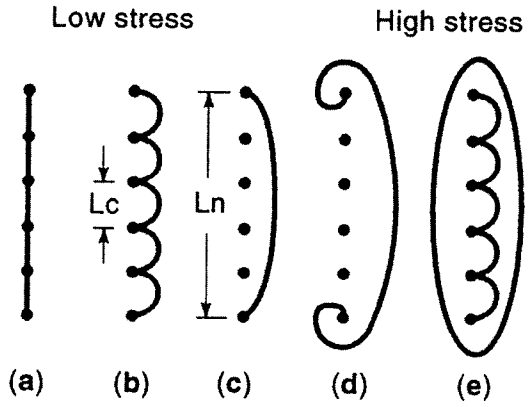

Figure 10. The successive drawings indicate schematically the bowing out of a pinned dislocation line by an increasing applied stress. As the stress increases, the loop L_C bow out until breakaway occurs. For very large stresses, the dislocations multiply according to Frank-Read mechanism.

If an external low stress is now applied (b), the loop (L_C) starts to bow out until the breakaway stress is reached. The effective modules of dislocation strain are determined by L_C in this range. At the breakaway stress (c), a large increase in the dislocation strain occurs. For further increasing of a stress the network length L_N bows out strongly and these external stresses are critical

for effective UST gettering. In fact, due to a dramatic increasing of the dislocation strain in (c-d), the additional impurities can be swept out from the bulk and captured at the Cottrell atmosphere around the dislocation. It is suggested that both the elastic strain and electric field of charged dislocation core are the driving forces in this UST gettering mechanism, contributing to the increase of the energy Q in Eq.(2). Further increase of applied stress provides a multiplication of dislocations according to the Frank-Read mechanism (e). Dislocation motion can be monitored by measuring the internal friction coefficient, which quantifies the value of dislocation ultrasonic damping. Internal friction study accesses the mechanical properties of a dislocation network such as density of pinning points, length of dislocation segments, and breakaway stress.

The illustrative example of UST defect gettering is shown in Figure 11 as two photoluminescence spectra measured at 4.2K in CdS single crystal before UST and after UST processing [14]. Low temperature excitonic PL spectroscopy is a convenient approach in selective monitoring of the concentration of point defects after various processing steps. Individual PL line corresponds to a particular point defect possessing a specific electronic level in the forbidden band. A variation of defect concentrations is ultimately reflected in the intensity of a corresponding excitonic PL line as compared to the PL intensity of other lines.

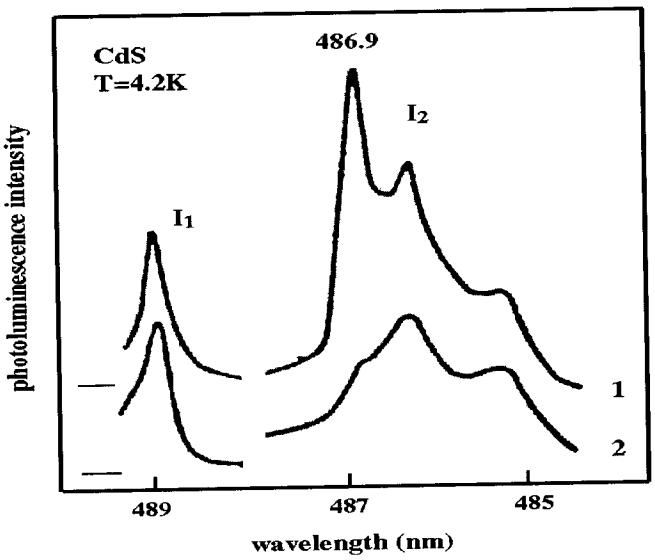

Figure 11. UST processing strongly reduces the concentration of shallow donors (interstitial Cd atoms) contributed to the intensity of 486.9nm PL line in CdS. This is shown as two photoluminescence spectra of the same CdS single crystal measured at T=4.2K before UST (1) and after UST (2).

In Figure 11, our concern is the intensity of two groups of excitonic lines: I_1 (acceptor bound exciton) and I_2 (donor bound exciton). The UST selectively reduces the intensity of the donor exciton at 486.9nm identified with interstitial Cd atoms. This UST process is caused by a gettering of shallow donors (Cd_i) by a dislocation network. The UST processing was applied at different temperatures below 100^0C using the internal piezoelectric effect of CdS as described in Chapter 1. It

was found , that the UST process is thermally activated exhibiting the activation energy close to the energy of shallow donor diffusion in CdS (~0.3eV). The PL spectroscopy data were approved by electrical measurements using thermally stimulated conductivity. They are also consistent with the data of internal fraction study: decreasing of the internal friction coefficient after UST observed in CdS single crystals [14]. Similar UST results were obtained with gettering of substitutional Li, Na, Cu and Ag in CdTe [15, 16]. It was concluded, that mobile point defects can be captured effectively by a dislocation network after UST processing. This result strongly suggests that the concentration of pinned points shown in Figure 10 was increased after UST processing, confirming the model of point defect gettering.

Dislocation gettering is closely related to another important UST phenomena: generation and multiplication of dislocations. In semiconductors a different type of dislocations - edge, screw, loop, and partial - are unavoidable growth and processing defects strongly influencing electronic properties of the material. On the other hand, promptly engineered dislocation network can benefit electronic materials, as was suggested, by using misfit dislocations in the SiGe/Si system [27]. In fact, the dislocations in the vicinity of an active region can be an excellent sink to capture residual impurities and to accomplish defect gettering. Direct measurement of dislocation density demonstrated dislocation multiplication in Ge single crystals after UST [11]. A fundamental study performed in II-VI compounds have shown that the gettering of acceptor mobile defects in CdTe – Li and Na - occurs after their diffusion and capture at "fresh" dislocations generated by ultrasound [16]. The dislocations were introduced using a short laser pulse and gettering was monitored as a conductivity decrease possessing the activation energy of point defect diffusion close to 0.15eV.

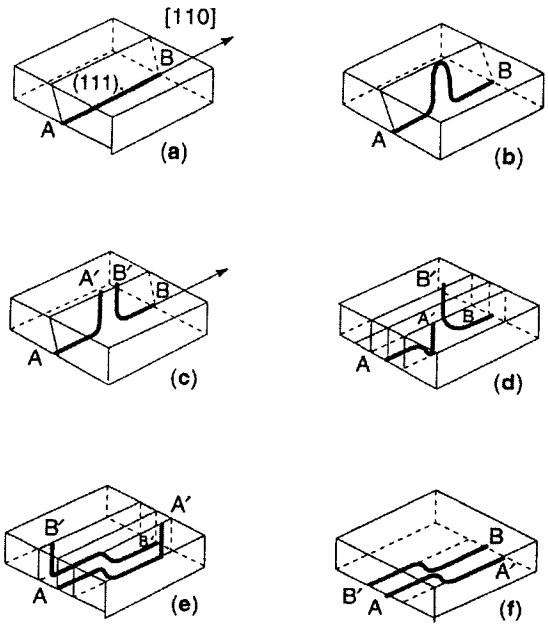

Figure 12. Schematic of consecutive stages of UST induced multiplication of the misfit dislocations at the hetero-boundary between a thin film and substrate.

Dislocations also provide a means to release a residual undesirable stress field at the misfit boundary between film and substrate. UST generation of dislocations occurs at relatively high UST density of power and is a result of a strong plastic deformation in crystal lattice. Within a string model described previously (Fig.2e), dislocations under strong UST stress can be released from some of its pinned points and a dislocation multiplication will occur.

The dislocation multiplication was directly observed using transmission electron microscopy in strained hetero layers composed of 0.2 μm to 5 μm Ge films deposited on the GaAs substrate [28]. By applying UST processing for 3 hours at 160kHz with the acoustic strain amplitude up to $2x10^{-4}$, it was found that UST promotes the glide and multiplication of existing dislocations in strained Ge/GaAs hetero structure. The following mechanism of a multiplication of misfit dislocations is schematically shown in Figure 12. Initially (fig.12a), a straight 60^0 misfit dislocation AB oriented along [110] direction is shown in the film-substrate boundary. Under UST, the dislocation dipole is formed in the (111) glide plane (fig.12b). This dipole can be broken by approaching a film surface (fig.12c), leaving two helical sections on the dislocation configurations AA' and BB'. The misfit stresses cause these sections to glide transversely (fig.12d) and also in planes parallel to the original glide plane (fig.12e), lengthening the misfit dislocation segments and subsequently relaxing misfit stresses. When the helical segments reach the edges of the film, the final pattern of two new misfit dislocations - AA' and BB' - is designed. This elementary process of a dislocation multiplication can be repeated under UST with AA' and BB' dislocations. Consequently, a misfit dislocation network can be engineered.

We notice that dislocations are usually considered as harmful defects to a semiconductor material or device. Therefore, special precautions have to be undertaken to avoid degradation of device performance after the dislocation network is created by UST.

3. Ultrasound driven metastability

Although UST effect was defined as a stable improvement of semiconductors and devices, a number of metastable phenomena mediated by the ultrasound have been observed. Metastability is a general property of defects in electronic materials, which are grown and processed under non-equilibrium conditions (doping, passivation, annealing, etc.). Applying low-amplitude ultrasonic vibrations to a system, one can perform non-destructive defect diagnostics by measuring post-UST relaxation of material characteristics and device parameters.

An illustrative example shows ultrasonic stimulated dissociation of Fe-B pairs in Cz-Si [7]. Contamination of commercial Si wafers with iron, even at the level of 10^{11} cm^{-3}, is detrimental for IC manufacturing. Therefore, a sensitive technique was developed for in-line control of Fe-contamination. This technique utilizes a method of surface photovoltage (SPV) to measure minority carrier diffusion length in the bulk of a semiconductor [29]. SPV is a non-contact, real-time method of quantitatively analyzing heavy metals in wafers. The technique uses light pulses directed onto the wafer to generate excess minority carriers. These carriers diffuse to the surface and change surface potential. A non-contact electrode placed above Si wafer surface senses the photovoltage, which is measured as a function of the light penetration depth into bulk silicon. The shorter the diffusion length, or higher the contamination, the faster the photovoltage is decreased with increasing light penetration depth. Although the SPV technique typically measures net contamination level, the Fe can be specifically identified using additional strong light illumination. This light from a lamp-source activates Fe by splitting the Fe-B pairs and eventually reducing the diffusion length from initial value (L_0) to a new one (L_1). According to a simple theory, the concentration of Fe-B pairs can be calculated as follows:

$$[FeB] = 1.05 \times 10^{16} \ (L_I^{-2} - L_I^{-2}) \ (cm^{-3}) \qquad (3)$$

For UST experiments, boron doped Cz-Si wafers were contaminated with iron at a concentration of 1.5×10^{14} cm^{-3}. This concentration was evaluated by means of an optical activation technique using Eq. (3). At room temperature in p-type material, the Fe is paired with doping acceptors (B) forming stable up to 200^0C nearest neighbor Fe-B pair, similar to the Cr-B pair in the previous section. UST performed at temperatures below 100^0C at 70kHz stimulates the process of Fe-B pair dissociation. This was controlled by reduction of minority carrier diffusion length measured with SPV technique as shown in Figure 13. It is important that 200^0C annealing of Si is required for thermal dissociation of Fe-B pairs. The UST enhanced dissociation is followed by a pairing of Fe and B due to a Colombic attraction of charged pair constituents and a fast diffusion of the interstitial Fe. Therefore, this UST triggered process is entirely reversible.

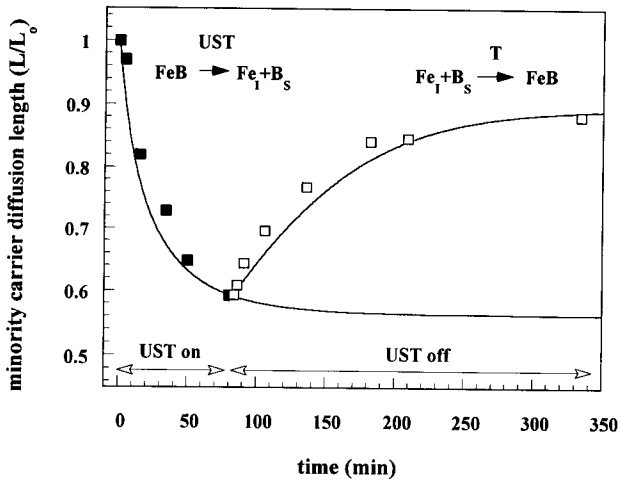

Figure 13. UST applied to p-type Cz-Si promotes breaking of Fe-B pairs. This process is monitored by a decreasing of minority carrier diffusion length. After ultrasound is turned off Fe and B are paired again, accomplishing the reversible dissociation/association process. UST breaking and pairing kinetics are measured at 75^0C.

This model case of Fe-B splitting under UST has the following explanation. A mobile Fe, bound with boron in the Fe-B pair, can exhibit a jumping from one interstitial position to a nearest equivalent one. The jumping rate is strongly stimulated when the frequency, f, of the applied ultrasonic vibrations is close to the resonance of pair reorientation followed by the equation:

$$2 \pi f = \nu_0 \exp (-U/kT_{UST}), \qquad (4)$$

where ν_0 is the lattice phonon frequency (typically of the order 10^{12} s^{-1}), T_{UST} stands for UST temperature, and U is the pair binding energy of the order of 0.5eV. It is easy to check that at 70kHz the Eq. (4) is fulfilled at 124^0C, which is close to the range of applied UST temperatures. The breaking of Fe-B pairs under UST occurs when the Fe atom approaches a saddle point between two equivalent interstitial sites: in this position a Colombic binding energy is substantially reduced, which promotes a dissociation of the pair components.

Metastable effects triggered by the UST processing were observed in II-VI materials [14,17,30]. After the UST was accomplished a long-term relaxation, measured at different temperatures, revealed diffusion of Cd interstitial atoms in CdS and shallow donors in ternary II-VI compounds. In this kind of experiment, UST dissociation - thermal association of pair centers and defect clusters, can be used for other heavy metal contamination (Cu, W, Cr) in Si for the purpose of their selective diagnostics.

4. Application of UST processing

UST technology has evident interest for various device applications. In Table 2 we summarized the results of UST application in various semiconductor devices. The upper-limit of UST effect shows the record of UST improvement of a device parameter. Some UST effects are indeed spectacular, while the others depict just a trend to follow-up research.

Table 2. Improvement of electronics devices using UST

Type of device	Material	Improved parameter	Upper limit of UST effect	Reference
Thin-film transistor	Poly-Si	Leakage current Threshold voltage	10 times lower 0.5V lower	[23]
Tunnel diode	GaAs	Current noise	4 times lower	[31]
Solar cell	Crystalline poly-Si	Efficiency	5% higher	[32]
Light emitting diode	InGaAs	Intensity	30% higher	[33]
	ZnS:Mn	Luminance	~2 times higher	[34]
IR detector	CdHgTe	1/f noise	10 times lower	[35]

To illustrate one of the UST applications, we present data on suppression of 1/f spectral density of noise observed in polycrystalline $Cd_{0.2}Hg_{0.8}Te$ [35]. This material is a recognized leader among infrared detectors for commercial and military applications. Samples were cut from the n-type $Cd_{0.2}Hg_{0.8}Te$ slab containing small-angle boundaries. The $Cd_{0.2}Hg_{0.8}Te$ lattice is characterized by a high concentration of mobile point defects such as Hg vacancies, defect precipitates in a form of HgTe and Te inclusions, dislocations, and small-angle grain boundaries. This complicated defect system appeared to be a proper object for the UST processing. The optimal UST effect was observed at an ultrasonic frequency in the range of 10 MHz, close to the characteristic vibration frequency of individual subblocks. The UST was performed at room temperature increasing the UST time from a few minutes to an hour. It is imperative to know that due to an extremely complicated combination of point and extended defects in a "soft" CdHgTe lattice, the UST effect is sensitive to experimental details, and even varies between samples cut from the same polycrystalline slab possessing different densities of small-angle grains boundaries. A dramatic, one order of

magnitude reduction of 1/f noise level (critical parameter of IR sensitivity) is very impressive and promising for IR applications.

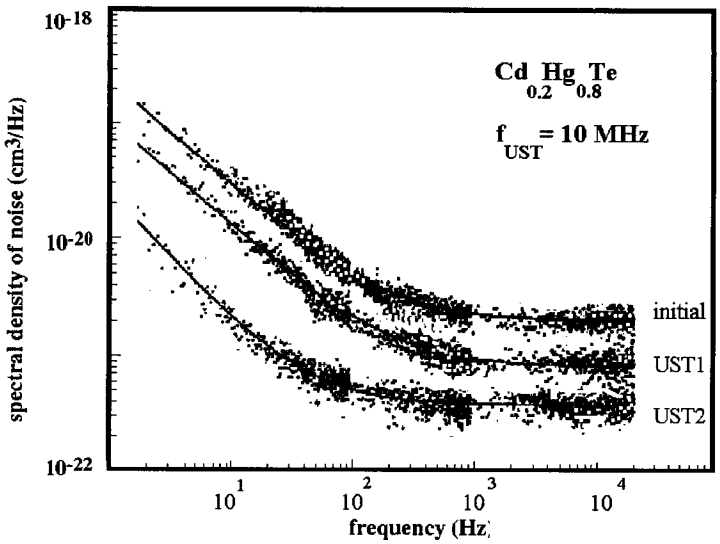

Figure 14. UST applied to CdHgTe ternary compound reduces the spectral density of 1/f noise by a factor of one order of magnitude (curve "UST2") compared to the initial state (curve "Initial").

Summary and conclusions

We have reviewed fundamental and application issues of the UST method in various semiconductors and electronic devices: single and compound materials; crystalline, polycrystalline, and amorphous; as-grown and processed wafers. Numerous ultrasonic-controlled defect reactions were observed and explored. Examples of a significant UST effect to enhance the point defect gettering and defect passivation with atomic hydrogen exhibit a strong potential for the UST technology to be utilized as a defect engineering tool.

After a comprehensive study, UST mechanisms enabled the development of a reliable methodology and apparatus for using the UST in microelectronics and optoelectronics. Feasibility projects performed on semiconductor devices established a statistically valid data-base for applying this technique to benefit device performance. Although the core of UST technology - a generation of the ultrasound into electronic material - is a common feature for various UST applications, a specific UST recipe has to be developed for each individual type of material or device. Such a recipe is comprised of a synergetic combination of the optimal UST parameters: temperature, amplitude, duration, and resonance frequency. Additionally, UST processing can be performed concurrently or consecutively with UV or IR light, under a pulsed electric field or laser activation, etc. This illustrates a high level of flexibility of the UST technology, its compatibility with different stages of a device fabrication, and an easy adjustment to a particular device problem.

Although the UST has not yet found a commercial niche in a broad variety of potential applications, one can predict that the time is coming to employ UST technology as an effective means for defect engineering in semiconductors.

References

1. A. P. Zdebskii, S. S. Ostapenko, A. U. Savchuk, and M. K. Sheinkman, Sov. Tech. Phys. Lett., **10** (1984) p. 525.
2. http://www.eng.usf.edu/CMR/smd/
3. A. P. Zdebskii, M. K. Sheinkman, A. N. Annaniyazov, and G. Garyagdyev, Sov. Phys. Solid state, **29** (1987), p.648.
4. L. V. Borkovskaya, B. R. Dzhumaev, I. A. Drozdova, N. E. Korsunskaya, I. V. Markevich, A. F. Singaevskii, and M. K. Sheinkman, Soviet Physics of Solid State, **37**, (1995) p. 1511.
5. S. Ostapenko, L. Jastrzebski, J.Lagowski, and R. K. Smeltzer: Appl. Phys. Lett., **68** (1996), p.2873.
6. Y. Koshka, S. Ostapenko, T. Ruf, and J. Zhang, Appl. Phys. Lett., **68** (1996), p. 2537.
7. S. Ostapenko and R. Bell, J. Appl. Phys, **77** (1995), p. 5458.
8. P. I. Baranskii, A. E. Belyaev, S. M. Komirenko, and N. V. Shevcenko, Sov. Phys. Solid State, **32** (1990), p. 1257.
9. V. L. Gromashevskii, V. V. Dyakin, E. A. Sal'kov, S. M. Sklyarov, N. S. Khilimova, Ukr. Fiz. Zhurnal, **29** (1984), p. 550.
10. A. Makosa, T. Wosinski, and Z. Witczak: Acta Physica Polonica A, **84** (1993), p. 653.
11. V. P. Grabchak and A. V. Kulemin: Sov. Phys. Acoust., **22** (1976), p. 475.
12. V. D. Krevchik, R. A. Muminov, and A. Ya. Yafasov: Phys. Stat. Sol. (a), **63** (1981), p. K159.
13. R. E. Bell, S. Ostapenko, and J. Lagowski, in "Defect and impurity engineered semiconductors and devices" (Material Research Society, Pittsburg, PA 1995), p.p 647 - 652.
14. P. Zdebskii, N. V. Mironyuk, S. S. Ostapenko, A. U. Savchuk, and M. K. Sheinkman: Sov.Phys.Semicond., **20** (1986), p. 1167.
15. V. N. Babentsov, S. I. Gorban', I. Ya. Gorodetckii, N. E. Korsunskaya, I. M. Rarenko, and M. K. Sheinkman: Sov. Phys. Semicond., **25** (1991), p. 749.
16. A. Baidullaeva, B. M. Bulakh, B. K. Dauletmuratov, B. R. Dzhumaev, N. E. Korsunskaya, P. E. Mozol', and G. Garyagdyev, Sov. Phys. Semicond., **26** (1992), p. 450.
17. G. Garyagdiev, I. Ya. Gorodetckii, B. R. Dzhumaev, N. E. Korsunskaya, I. M. Rarenko, and M. K. Sheinkman: Sov. Phys. Semicond., **25** (1991), p. 248.
18. G. Garyagdyev, I. Ya. Gorodetskii, B. R. Dzhumaev, N. E. Korsunskaya, and K. Nurmukhametov, Ukr. Fiz. Zhurnal, **34** (1989), p.1553.
19. S. Ostapenko, Materials Science Forum, **258-263** (1997), p. 197.
20. A. U. Savchouk, S. Ostapenko, G. Nowak, J. Lagowski, and L. Jastrzebski: Appl. Phys. Lett, **67** (1995), p. 82.
21. N.H.Nickel, N.M.Johnson, and W.B.Jackson: Appl.Phys.Lett., **62** (1993), p.3285.
22. A. Van Wieringen and N. Warmoltz, Physica **22** (1956), p. 849.

23. S. Ostapenko, L. Jastrzebski, J. Lagowski, and R.K. Smeltzer: MRS Symposium Proceedings, **424** (1997), p. 201.
24. V. M. Golikov, A. V. Kulemin, V. A. Lazarev, and V. P. Manaenkov, Soviet Physics - Acoustics, **21** (1975), p. 524.
25. V. N. Pavlovich: Phys. Stat. Sol. (b), **180** (1993), p. 97.
26. A.V.Granato and K.Lucke, in Physical Acoustics, ed.by W.P.Mason, **4A** (1966), pp.225-276.
27. F. Shimura, Semiconductor silicon crystal technology. (San Diego, CA: Academic Press, Inc.) pp.: 344-377 (1989).
28. V. F. Britun, N. Ya. Gorid'ko, V. L. Korchnaya, G. N. Semyonova, M. Ya. Skorohod, Yu. A. Thorik, L. S. Khazan, and M. K. Sheinkman, Sov.Phys. Solid State, **33** (1991), p. 1317.
29. J. Lagowski, P.Edelman, M. Dexter, and W. Henley, Semicon. Sci. Technol., **7** (1992), p. A185.
30. P. Zdebskii, N. V. Mironyuk, S. S. Ostapenko, L. N. Khanat, and G. Garyagdyev, Sov.Phys.Semicond., **21** (1987), p. 570.
31. P. Zdebskii, M. I. Lisyanskii, N. B. Luk'yanchikova, and M. K. Sheinkman: Sov. Tech. Phys. Lett., **13** (1987), p. 421.
32. Iskanderov, V. D. Krevchik, R. A. Muminov, and I. U. Shadybekov: Applied Solar Energy, **24** (1988), p. 21.
33. P. Zdebskii, V. L. Korchnaya, T. V. Torchinskaya, and M. K. Sheinkman: Sov. Tech. Phys. Lett, **12** (1986), p. 31.
34. V. G. Akul'shin, V. V. Dyakin, V. N. Lysenko, and V. E. Rodionov: Sov. Phys. Tech. Phys. **34** (1989), p. 1186.
35. Ya. M. Olikh and Yu. N. Shavlyuk: Phys. Solid State, **38** (1996), p. 1835.

Defect Interaction and Clustering in Semiconductors
10.4028/www.scientific.net/SSP.85-86

Ultrasound Stimulated Defect Reactions in Semiconductors
10.4028/www.scientific.net/SSP.85-86.317